

A novel autoencoder approach with rescaling transformation distance metric for feature extraction to high-dimensional data

Jian Zheng¹, Hongchun Qu^{Corresp., 1, 2}, Zhaoni Li¹, Lin Li¹, Xiaoming Tang², Fei Guo²

¹ College of Computer Science and Technology, Chongqing University of Post and Telecommunications, Chongqing, China, China

² College of Automation,, Chongqing University of Posts and Telecommunications,, chongqing, China, China

Corresponding Author: Hongchun Qu
Email address: hcchy@gmail.com

Feature extraction usually needs to rely on sufficient information of the input data, unfortunately, the distribution of the data upon a high-dimensional space is too sparse to provide sufficient information for feature extraction. Moreover, high dimensionality of the data also brings trouble for the searching of those features scattered in subspaces. As such, it is a tricky work for feature extraction from the data in a high-dimensional space. To address this issue, this paper proposes a novel autoencoder approach based on Mahalanobis distance metric of rescaling transformation. Through performing rescaling transformation on Mahalanobis distance metric, then the transformed Mahalanobis distance metric is introduced into the autoencoder, so as to improve the ability of feature extraction to the model. Results show that the proposed approach wins comparison methods in terms of both the accuracy of feature extraction and the linear separabilities of the extracted features. We indicate that distance metric-based methods are more suitable for extracting those features with linear separabilities from high-dimensional data than feature selection-based methods. In a high-dimensional space, evaluating feature similarity is relatively easier than evaluating feature importance, so that distance metric methods by evaluating feature similarity gain advantages over feature selection methods by assessing feature importance for feature extraction, while the latter is higher than the former in terms of computational efficiency.

1 A novel autoencoder approach with rescaling
2 transformation distance metric for feature extraction to
3 high-dimensional data

4

5

6 Jian Zheng ¹, Hongchun Qu^{1,2,*}, Zhaoni Li ¹, Lin Li¹, Xiaoming Tang ², Fei Guo²

7

8 ¹ College of Computer Science and Technology, Chongqing University of Posts and
9 Telecommunications, Chongqing, 400065, China

10 ² College of Automation, Chongqing University of Posts and Telecommunications, Chongqing,
11 400065, China

12

13

14 Corresponding Author:

15 Hongchun Qu

16 Congwenlu Road, Chongqing, 400065, China

17 Email address: hcchu@gmail.com

18

19

20 **Abstract**

21 Feature extraction usually needs to rely on sufficient information of the input data, unfortunately,
22 the distribution of the data upon a high-dimensional space is too sparse to provide sufficient
23 information for feature extraction. Moreover, high dimensionality of the data also brings trouble
24 for the searching of those features scattered in subspaces. As such, it is a tricky work for feature
25 extraction from the data in a high-dimensional space. To address this issue, this paper proposes a
26 novel autoencoder approach based on Mahalanobis distance metric of rescaling transformation.
27 Through performing rescaling transformation on Mahalanobis distance metric, then the
28 transformed Mahalanobis distance metric is introduced into the autoencoder, so as to improve the
29 ability of feature extraction to the model. Results show that the proposed approach wins
30 comparison methods in terms of both the accuracy of feature extraction and the linear
31 separabilities of the extracted features. We indicate that distance metric-based methods are more
32 suitable for extracting those features with linear separabilities from high-dimensional data than
33 feature selection-based methods. In a high-dimensional space, evaluating feature similarity is
34 relatively easier than evaluating feature importance, so that distance metric methods by
35 evaluating feature similarity gain advantages over feature selection methods by assessing feature
36 importance for feature extraction, while the latter is higher than the former in terms of
37 computational efficiency.

38

39 Keyword: Autoencoder, Distance metric, Feature extraction

40 Introduction

41 High-dimensional data usually contains rich features, through extracting the important features,
42 those irrelevant attributes in high-dimensional data can be filtered, thereby achieving data
43 dimensionality reduction (*Xue et al., 2015*). Hence, feature extraction is considered to be one of
44 the important methods for data dimension reduction (*Bo et al., 2016*).

45 Feature extraction is a hot topic in recent years, aiming to gain the most valuable features from
46 the input data (*H.Tao et al., 2016; M. Luo et al., 2018*). High dimensionality of data, the so-
47 called the curse of dimensionality, brings negative effects for feature extraction (*J.Gui et al.,*
48 *2018; R. Chakraborty, N.R.Pal, 2015*). Upon a low-dimensional space, those relations between
49 the data are relatively compact but they may become sparse upon a high-dimensional space (*Bing*
50 *et al., 2021*), e.g., the data space with more than 10 dimensionalities (*A.-M., et al, 2011*). Clearly,
51 sparse relations between data are usually considered to be an unfavorable factor for feature
52 extraction since feature extraction needs to rely on the relations between data (*Bo et al., 2021*).
53 Beyond that, those latent features scattered in subspaces inside a high-dimensional space not
54 only inspect the ability of methods to extract features (*L. Wang et al., 2016*), but also test their
55 extraction efficiency. Hence, it is a challenge for feature extraction from high-dimensional data.

56 Recently, some opinions have been proposed for feature extraction, for instance, distance
57 metric-based methods, where, the typical representative is the well-known Mahalanobis distance-
58 based methods, which evaluates the similarity between samples using the covariance matrix of
59 data (*R. De et al, 2000*). Furthermore, *S.-Y (2018)* et al proposed the intrinsic semi-supervised
60 metric learning (ISSML) based on a distance metric for feature extraction. Similar, the methods
61 implemented in (*P. Zadeh et al, 2016*) and (*H. Luo, 2017*) also applied distance metrics.
62 Certainly, also including, the information-theoretic metric learning is (ITML) (*J. Mei et al, 2014*)
63 employed a distance metric to obtain features. These methods in (*S. Ying et al, 2018; P. Zadeh et*
64 *al, 2016; H. Luo, 2017; J. Mei et al, 2014*) address the issues of symmetric positive-definite
65 matrix minimization during feature extraction, but there are several problems in them, 1) since
66 most of them use iterative calculation while performing feature selection, optimization issues
67 have to be addressed iteratively. 2) Most of them need to rely on parameter selection to obtain
68 those desired features. Usually, feature selection-based methods are also considered to be used
69 for feature extraction. Such methods achieve feature extraction through analyzing the
70 information of feature subsets, for example, the cheap feature selection method based on *k*-
71 means algorithm (*Marco et al, 2021*) selects the *m* features with the highest relevance measure
72 through obtaining a clustering for each subset of features. Although the method (*Marco et al,*
73 *2021*) is a novel measurement for feature relevance, which is beneficial for feature selection,
74 however, calculating per subset of features needs to spend a lot time cost. In order to reduce the
75 correlation between features, some measurements for quickly assessing features are proposed,
76 e.g., the information entropy metric (*T. X. et al, 2019*), whereas the method (*T. X. et al, 2019*) has
77 a bias toward features, which may result in appearing selecting deviation during feature
78 extraction. Another kind of feature selection method depends on eigen decomposition, such as,
79 locally linear embedding (LLE) (*R. Hettiarachchi, J. F. Peters, 2015; Ugochukwu Ejike Akpudo,*

80 *Jang-Wook Hur, 2020*), multi-manifold discriminant isometric feature mapping (MMD-
81 ISOMAP) (*Bo.Y et al, 2016*), ISOMAP-KL (*Alaor Cervati Neto, Alexandre L. M. Levada, 2020*),
82 however, they cannot assess the importance of the features in the background space explicitly.

83 Neural network-based methods are favored because of excellent feature capture ability
84 (*Hong.C et al, 2022*), e.g., Multilayer Perceptron Neural Network (*K. Sun et al., 2017*). For
85 dimension reduction, feature extraction and data compression, autoencoder-based networks
86 provide an interpretable approach for the unknown meaningful insights (*Ang et al., 2017*) by
87 learning non-identity mapping functions (*Jian et al., 2022*), for instance, *Rami et al (2022)*
88 developed interpretable data representation for data dimensionality reduction using Logic-
89 Oriented and Granular Logic Autoencoders, and such as, Autoencoder (*Angshul Majumdar,*
90 *2019*) for image compression, and Blind Denoising autoencoder (*Fei et al, 2020*) for denoising.
91 In addition, sparse autoencoders are used as an unsupervised feature extractor to serve data
92 dimensionality reduction, feature extraction and data mining (*Z.Qiang et al., 2018*), e.g., *K.-J et*
93 *al (2018)* proposed Sparse Autoencoder (SAE) for feature extraction of ferroresonance
94 overvoltage waveforms in power distribution systems.

95 In this study, our motivation is to extract the features with linear separabilities from the data in
96 a high-dimensional space. Thus, we proposed a novel autoencoder method based on Mahalanobis
97 distance metric of rescaling transformation. The proposed method does not have to address any
98 optimization issue, and also it can focus on the whole data distribution.

99 We summarize the main contributions of this work as follows:

100 (i) Distance metric-based methods are more suitable for extracting those features with linear
101 separabilities from high-dimensional data than feature selection-based methods.

102 (ii) Assessing feature similarity in a high-dimensional space is relatively easier than evaluating
103 feature importance, therefore, distance metric approaches by evaluating feature similarity have
104 more advantages than feature selection approaches by evaluating feature importance in terms of
105 feature extraction.

106 (iii) The computational time of distance metric-based algorithms is higher than that of feature
107 selection-based algorithms upon a high-dimensional space.

108 This paper is organized as follows. Section 2 describes the proposed method and implements
109 the proposed model, including training for the model and parameter configuration. Experiment
110 datasets, competing methods, and experiment description are given in Section 3. Section 4
111 presents experiment results. Section 5 draws conclusions.

112

113 **Methods**

114 **Theory**

115 Given a sample $X = \{x_i | 1 \leq i \leq N\}$, and $X \subseteq \mathbb{R}^d$. \mathbb{R}^d is the d -dimensional Euclidean space. P is the
116 probability distribution of X , denoted as original probability distribution. $u(X)$ and Γ_x are the
117 mean vector and the covariance matrix of X , respectively. Let us assume that $Z = \{z_j | 1 \leq j \leq N\}$ is
118 the reconstructed X , and $Z \subseteq \mathbb{R}^d$. Q is the probability distribution of Z , denoted as approximate

119 probability distribution. Similar, $u(Z)$ and Γ_z are the mean vector and the covariance matrix of Z ,
 120 respectively. The K-L divergence (D. Tao et al, 2009) between the two distributions P and Q is
 121 given in Eq. (1).

$$122 \quad K(P \parallel Q) = \frac{1}{2} \left[\log |\Gamma_z| - \log |\Gamma_x| + \text{tr}(\Gamma_z^{-1} \Gamma_x) + \text{tr}(\Gamma_z^{-1} D_{xz}) \right] \quad (1)$$

123 Where $|\Gamma| = \det(\Gamma)$. The $\text{tr}(\bullet)$ is the trace of a matrix. $D_{xz} = (u(X) - u(Z))(u(X) - u(Z))^T$ is a symmetrical
 124 matrix. Training a distance metric is equivalent to finding a rescaling of a sample which replaces
 125 each x_i with $M^T x_i$ (Lin et al, 2019), so the K-L divergence in Eq. (1) can be converted into Eq.
 126 (2), having

$$127 \quad K_L^*(P \parallel Q) = \frac{1}{2} \left[\log |M^T \Gamma_z M| - \log |M^T \Gamma_x M| + \text{tr}((M^T \Gamma_z M)^{-1} (M^T (\Gamma_x + D_{xz}) M)) \right] \quad (2)$$

128 Where M is a metric matrix and satisfies $A^* = MM^T$, and $M \in \mathfrak{R}^{d \times d_0}$, $d_0 \leq d$. The K-L divergence in
 129 Eq. (2) is the rescaling transformation for the K-L divergence in Eq. (1) using the distance metric
 130 matrix A^* . To reduce the difference between the approximate distribution Q and the original
 131 distribution P , we consider Mahalanobis distance metric for K-L divergence in Eq. (2), having

$$132 \quad K-L(d_{A^*}) = K_L^*(P \parallel Q) + \sum_{1 \leq i, j} d_{A^*}(x_i, z_j) \quad (3)$$

133 $d_{A^*}(x_i, z_j)$ is Mahalanobis distance between x_i and z_j using A^* . The advantage of doing this is that
 134 the Mahalanobis distance using A^* can appropriately measure similarities between the input
 135 sample and the reconstructed input sample because of non-negativity (i.e., $d_{A^*}(x_i, z_j) \geq 0$),
 136 distinguishability (i.e., $d_{A^*}(x_i, z_j) = 0 \Leftrightarrow x_i = z_j$) and symmetry (i.e., $d_{A^*}(x_i, z_j) = d_{A^*}(z_j, x_i)$) (Lin et al,
 137 2019). Eq. (4) gives the calculation of $d_{A^*}(x_i, z_j)$, where A^* can be decomposed as $A^* = MM^T$.

$$138 \quad d_{A^*}(x_i, z_j) = \sqrt{(x_i - z_j)^T A^* (x_i - z_j)} \quad (4)$$

139 Model implementation

140 A classic auto encoder (AE) consists of an input layer, a hidden-layer and an output layer. For
 141 AE, the loss error is often measured by using the distance between the original input instance, the
 142 predicted instances, and the reconstructed instance (L. Theis et al, 2017). Usually, using
 143 divergence metrics or expanding autoencoder structures (e.g., enlarging the number of hidden
 144 layers) is more helpful for autoencoders to characterize the data distribution and to learn the
 145 desired representations (Weining et al, 2017). As such, we designed an autoencoder with
 146 multiple-hidden layers, namely m-AE, and $m \geq 1$, as shown in Fig.1. In addition, the K-L
 147 divergence in Eq. (3) was used to increase the ability of m -AE to capture low-dimensional
 148 feature representations. The loss error $\nabla_{KL}(\mathbf{w}, \mathbf{b})$ in m -AE is given as follows:

$$150 \quad \nabla_{KL}(\mathbf{w}, \mathbf{b}) = \sum \|e_x - e_z\|^2 + K-L(d_{A^*}) \quad (5)$$

151 Where e_x, e_z are the inputting and the reconstructed inputting, respectively. $\nabla_{KL}(\mathbf{w}, \mathbf{b})$ is updated
 152 through using the backpropagation manner.

153

154 To better train the proposed model, we carefully studied part hyper parameters in the model.
155 For the rest of hyper parameters, their default values were used.

156 (i) Optimizer. Common optimizers are Adam, RMSprop, SGD, Momentum, Nesterov, etc.
157 However, we selected Adam as the optimizer of m-AE, since Adam has the ability to handle
158 sparse gradients (Diederik P. Kingma, Jimmy Lei Ba, 2015). Compared with other optimizers,
159 Adam is more suitable for high-dimensional data. Moreover, Adam can provide different
160 adaptive learning rates for different hyper parameters.

161 (ii) Activation function. Gradient vanishing is easily to be induced during passing gradients
162 backwards for neural networks, in this case, the probability of gradient vanishing caused by
163 activation function Sigmoid is relatively high. Similar to Sigmoid, activation function tanh also
164 suffers from this problem. While for activation function ReLu, the phenomenon of gradient
165 vanishing is partially alleviated, meaning that gradient vanishing does not appear in the positive
166 interval of ReLu. Furthermore, ReLu converges much faster than Sigmoid and Tanh. Therefore,
167 we chose ReLu as the activation function of m-AE.

168 (iii) Iteration epoch. We dynamically adjust the iteration epoch according to training accuracy.
169 For instance, when training accuracy starts to change from large to small, we reduce iteration
170 epoch in order to prevent over-fitting. When the difference in accuracy between training and
171 testing is minimal, the current iteration epoch can be accepted and training procedure is stopped.

172 We give the training algorithm for m-AE in Algorithm 1. In the algorithm, the training set
173 $Train_set$ is divided into two datasets T^{Cro_train} , T^{Cro_val} in step 1. Since m-AE has multiple hidden
174 layers, we set m in the range of O_m , in order to determine the m , the dataset T^{Cro_train} is used to
175 train m-AE. The data set T^{Cro_val} is used for the validation of the network structure of m-AE. To
176 get the optimal m , denoted as m_{opt} , the cross-validation is implemented in step 2 to step 18,
177 where the procedure of step 6 and step 10 describes the calculation process of loss error $\nabla_{kl}(\mathbf{w}, \mathbf{b})$.
178 After gaining the optimal m , m-AE is trained using the training set $Train_set$. Using
179 backpropagation manner updates network parameters until m-AE can converge, as shown in step
180 18 to step 28. The procedure shown in step 29 to step 33 indicates that the maximum training
181 accuracy $Train_acc$ are outputted and the well trained m-AE is saved.

182

183

184 **Algorithm 1.** Training for m-AE.

185 Input: Training set $Train_set$, $A^* = I \in \mathbb{R}^{d \times d}$ is an identity matrix, iteration epoch T , L , parameter
186 O_m .

187 Output: Training accuracy $Train_acc$.

188 **Begin:**

189 1. $Train_set$ is divided into T^{Cro_train} , T^{Cro_val} ;

190 2. **for** $t=1$ to T **do:**

191 3. **foreach** m **in** O_m :

192 4. Decompose A^* as satisfying $A^* = MM^T$ using eigen decomposition.

193 5. Calculate loss error $\nabla_{KL}(\mathbf{w}, \mathbf{b})$ using Eq. (5) and the procedure is summarized as
 194 following:
 195 6. The procedure:
 196 7. Calculate $K_L^*(P \parallel Q)$ using Eq. (2).
 197 8. Calculate $d_{A^*}(x_i, z_j)$ using Eq. (4).
 198 9. Take $K_L^*(P \parallel Q)$ and $d_{A^*}(x_i, z_j)$ into Eq. (3) to calculate $K-L(\delta_{A^*})$.
 199 10. For any x_i, x_j , calculate $\nabla_{KL}(\mathbf{w}, \mathbf{b})$ using Eq. (5).
 200 11. Calculate training accuracy $T_acc = m\text{-AE}(T^{Cro_train}, m; t)$;
 201 12. Validate m-AE using data set T^{Cro_val} ;
 202 13. Calculate validation accuracy $V_acc = m\text{-AE}(T^{Cro_val}, m; t)$
 203 14. Update weight $\mathbf{w} \leftarrow \mathbf{w} + \nabla \mathbf{w}$.
 204 15. Update A^* as MM^T .
 205 16. Until A^* and hyper parameters converge.
 206 17. **end foreach**
 207 18. **end for**
 208 19. Get the optimal value of m , i.e., $m_{opt} = \arg \max(V_acc)$;
 209 20. **for** $l=1$ **to** L **do**:
 210 21. Decompose A^* as satisfying $A^* = MM^T$ using eigen decomposition.
 211 22. Train m-AE using training set $Train_set$ and m_{opt} ;
 212 23. Update network parameters using the optimizer Adam ;
 213 24. Calculate loss error $\nabla_{KL}(\mathbf{w}, \mathbf{b})$ using Eq. (5);
 214 25. Calculate training accuracy $Training_acc(l) = m\text{-AE}(Train_set; m_{opt})$;
 215 26. Update A^* as MM^T ;
 216 27. Using backpropagation manner updates network parameters;
 217 28. **end for**
 218 29. Select the l so that $l_{max} = \arg \max(Training_acc(l))$;
 219 30. Get the maximum training accuracy $Train_acc$ in the l_{max} -th iteration ;
 220 31. $Train_acc = m\text{-AE}(Train_set; m_{opt}, l_{max})$;
 221 32. Output $Train_acc$
 222 33. Save the well trained m-AE($Train_set; m_{opt}, l_{max}$);
 223 **End**

224
 225

226 EXPERMENTS

227 Datasets and assessment metrics

228 To verify the performance of the proposed m-AE, we selected 4 benchmark datasets with
 229 different data dimensions from the UCI machine learning repository (*C. L. Blake, C. J. Merz,*
 230 *1998*). The attributes of the 4 benchmark datasets are summarized in Table 1.

231 Receiver operating characteristic curve (ROC) and corresponding area under curve (AUC) are
232 usually used to assess the precision of machine learning methods. Therefore, AUC is taken as the
233 assessment metric of method precision.

234

235 **Competing and benchmark methods**

236 Since m-AE applies the distance metric of rescaling transformation, the methods based on a
237 distance metric were used for comparisons, including ISSML (*S.-Y et al, 2018*) and ITML (*J.
238 Mei et al, 2014*). Certainly, the method based on feature selection was also considered, i.e.,
239 MMD-ISOMAP (*Bo.Y et al, 2016*). In addition, autoencoder-based approaches were used as a
240 comparison, e.g., the SAE (*K.-J et al, 2018*). Furthermore, to further examine the effects of the
241 distance metric of rescaling transformation on the performance of m-AE, a benchmark model
242 was developed with m-AE as a reference. The developed benchmark model used the same
243 structure and parameter configuration of m-AE without using the distance metric of rescaling
244 transformation, namely AE-BK.

245 We implemented the corresponding algorithms of the six models using Python on Tensorflow
246 framework. While for those parameters of competing methods, we adopted those values
247 observed in the corresponding literature. Certainly, unless otherwise stated, the five
248 corresponding algorithms all run on the same GPU and apply the same experimental
249 configuration settings.

250

251 **Experiment description**

252 Experiments were conducted on the four benchmark datasets in order to validate the ability of
253 these six models to extract features and their efficiency.

254 **Experiment I.** To test the robustness of m-AE. The proposed m-AE has multiple hidden
255 layers, since the number of hidden layers (i.e., the m) significantly affects the precision of feature
256 extraction, the m needs to be firstly verified, i.e., robustness testing of the model, let m set in the
257 range of $\{1, 2, 3, 4, 5, 7, 10, 15, 20\}$.

258 **Experiment II.** To test the ability of feature extraction for the six models. The six models
259 were run on the four benchmark datasets, and then the testing results were analyzed.

260 **Experiment III.** To compare the efficiency of our method with competing methods. These
261 methods were performed on four benchmark datasets and observed their running time.

262 **Ablation experiments.** To verify that using the distance metric of rescaling transformation
263 can be beneficial for extracting linearly separable features, the ablation experiments were also
264 designed.

265 In addition, to eliminate randomness during the experiment and present an objective result,
266 we used cross-validation to verify the six models. We randomly selected two datasets from the
267 four benchmark datasets as the training set to train the six models. Once the six models were well
268 trained, they were tested on the four benchmark datasets, respectively. The process was repeated
269 five times, independently, then we took the average of five testing results as a measurement.

270

271 **RESULTS**

272 **Experiments on robustness**

273 Results in Fig.2 and Fig.3 show that the performance of the proposed m-AE and the benchmark
274 model AE-BK improves along with increasing of m , and then the performance remains stable
275 when m reaches a certain size, i.e., $m=3$. This means that m-AE and AE-BK are not sensitive to
276 large m on the four benchmark datasets, i.e., their network structures are robust within a
277 reasonable range. Therefore, let m be equal to 3 in subsequent experiments.

278

279 **Comparisons of accuracy extraction**

280 Results in Table 2 show that the proposed m-AE wins the four competing models and the
281 benchmark model in the accuracy of feature extraction on all considered instances. For
282 competitors, ISSML, ITML and SAE outperform MMD-ISOMAP in most benchmark datasets
283 for the extracted accuracy.

284

285 **Comparisons of linear separability.**

286 The results of ablation experiments in Fig.4 show that compared with the models without using
287 distance metrics, e.g., AE-BK, SAE, the models using distance metrics (including m-AE,
288 ISSML, ITML) perform much better on most datasets in the extracted accuracy of the features
289 with linear separabilities. Similar, the models using distance metrics also win the model using
290 feature selection, as shown in Fig.5. To observe the linear separabilities of the extracted features
291 from the four benchmark datasets, we projected these extracted features onto 2-dimensional
292 space, and then visualized them. Fig.6 displays the results of visualized distribution on the four
293 benchmark datasets by the six models. The visualized results show that it is optimal for the
294 separation distance between different types of features extracted by m-AE, meaning that
295 compared with competing and benchmark models, m-AE is a winner in terms of the linear
296 separabilities of the extracted features. Together, these results imply that distance metric-based
297 methods have advantages over feature selection-based methods in terms of extracting the
298 features with linear separabilities.

299

300 **Running time**

301 Fig.7 displays the running time of methods. Obviously, the advantage of m-AE in running time is
302 not as significant as that in both the extracted accuracy and the linear separabilities of the
303 extracted features. MMD-ISOMAP spends less in running time on most benchmark datasets than
304 distance metric-based methods, meaning that the execution efficiency of feature selection-based
305 methods is higher than that of distance metric-based methods when running upon a high-
306 dimensional space. Distance metric-based methods take a lot of time to calculate the distance
307 between each point pair upon a high-dimensional space, so as to increase the running time.

308

309 **Discussion**

310 Compared with the competitors, the proposed m-AE has outstanding advantage in term of both

311 the accuracy of feature extraction and the linear separabilities of the extracted features on high-
312 dimensional data. We interpret it as following. On one hand, Mahalanobis distance in Eq. (3)
313 can appropriately measure similarities between the input sample and the reconstructed input
314 sample, so as to minimize the loss error of m-AE in Eq. (5). As such, m-AE gains the desired
315 accuracy of feature extraction. On the other hand, we performed a rescaling on K-L divergence
316 metric in Eq. (2) by using A^* in Eq. (4), which effectively allows the extracted features to present
317 linear separabilities, because the rescaling can maximized the classification distance between the
318 extracted different types of features. Hence, the features extracted by m-AE present linear
319 separabilities than competitors .Overall, m-AE outperforms the competitors in extracted accuracy
320 and the linear separabilities of the extracted features.

321 In a high-dimensional space, distance metric-based methods easily evaluates the feature
322 similarity by calculating the distance between the data, however, feature selection-based methods
323 relatively difficulty assess the feature importance. Therefore, distance metric-based methods, e.g.,
324 ISSML (*S.-Y et al, 2018*) and ITML (*J. Mei et al, 2014*), are more suitable for extracting those
325 low-dimensional features with the linear separability from high-dimensional data than feature
326 selection-based methods. However, the computational time of feature selection-based methods,
327 e.g., MMD-ISOMAP (*Bo.Y et al, 2016*), is lower than that of distance metric-based methods in a
328 high-dimensional space, since distance metric-based methods spend too much in calculating the
329 distance between each point pair.

330 Although autoencoders have excellent feature capture capabilities, they may perform poorly in
331 extracting linearly separable features, e.g., SAE (*K.-J et al, 2018*). Whereas, this deficiency of
332 autoencoders can be remedied by introducing a distance metric. Certainly, there are many
333 methods of distance metrics, e.g., Wasserstein distance metric (*Na et al, 2019; Jian et al, 2022*),
334 Bhattacharyya distance metric (*Mariucci E, Reiß M, 2017*).

335

336 **Conclusions**

337 This paper proposed a novel autoencoder method based on Mahalanobis distance metric of
338 rescaling transformation to extract low-dimensional features from the data in the high-
339 dimensional space. Results on show that compared with competing methods, the proposed
340 method is a winner in both the accuracy of feature extraction and the linear separabilities of the
341 extracted features. We find that the linear separabilities of those features obtained by the distance
342 metric-based methods are better than that of obtained by the feature selection-based methods.
343 Compared with feature selection-based methods, distance metric-based methods have more
344 advantages for low-dimensional feature extraction, however, feature selection-based methods are
345 higher than that of distance metric-based methods in terms of computational efficiency.

346

347 **Funding**

348 The funding received from the National Natural Science Foundation of China under grant
349 #61871061

350

351 Data availability

352 The datasets in this work can be found at <http://archive.ics.uci.edu/ml/>

353

354 Competing interests

355 The authors declare no conflict of interest.

356

357 References

- 358 **Alaor Cervati Neto, Alexandre L. M. Levada. 2020.** ISOMAP-KL: a parametric approach for
359 unsupervised metric learning. *2020 33rd SIBGRAPI Conference on Graphics, Patterns and*
360 *Images (SIBGRAPI)*. 1-1.
- 361 **A.-M. Zhou, K. D. Kumar, Z.-G, Hou. 2011.** Finite-time attitude tracking control for
362 spacecraft using terminal sliding mode and Chebyshev neural network. *IEEE Trans. Syst.,*
363 *Man, Cybern. B, Cybern.* **41(4)**:950-963.
- 364 **Ang Jun Chin, Andri Mirzal, Habibollah Haron. 2016.** Supervised, Unsupervised and Semi-
365 supervised Feature Selection: A Review on Gene Selection. *IEEE Transactions on*
366 *Computational Biology and Bioinformatics* **13(5)**:971-989
- 367 **Angshul Majumdar. 2019.** Blind Denoising Autoencoder. *IEEE Transactions on Neural*
368 *Networks and Learning Systems* **30(1)**:312-317.
- 369 **Bing Tu, Xiaolong Liao, Chengle Zhou. 2021.** Feature Extraction Using Multitask Superpixel
370 Auxiliary Learning for Hyperspectral Classification. *IEEE Transactions on Instrumentation*
371 *and Measurement* **70**:1-16.
- 372 **Bo Peng, Shuting Wan, Ying Bi. 2021.** Automatic Feature Extraction and Construction Using
373 Genetic Programming for Rotating Machinery Fault Diagnosis. *IEEE Transactions on*
374 *Cybernetics* **51(10)**:4909-4923
- 375 **Bo Tang, Steven Kay, Haibo He. 2016.** Toward Optimal Feature Selection in Naive Bayes for
376 Text Categorization. *IEEE Transactions on Knowledge and Data Engineering* **28(9)**:2508-
377 2521.
- 378 **Bo. Yang, M. Xiang, Y. Zhang. 2016.** Multi-manifold discriminant isomap for visualization and
379 classification. *Pattern Recognition* **55**:215-230.
- 380 **C. L. Blake and C. J. Merz. 1998.** UCI Repository of Machine Learning Databases,
381 Department of Information and Computer Science. [Online]. Available: <http://www.ics.uci.edu/ml/learn/MLRepository.html>
- 382
- 383 **Diederik P. Kingma, Jimmy Lei Ba. 2015.** Adam: A method for stochastic optimization. arXiv
384 preprint. arXiv:1412.6980v8.
- 385 **D. Tao, X. Li, X. Wu, S. J. Maybank. 2009.** Geometric mean for subspace selection. *IEEE*
386 *Transactions on Pattern Analysis and Machine Intelligence* **31(2)**:260-274.
- 387 **Fei Yang, Luis Herranz, Joost van de Weijer. 2020.** Variable Rate Deep Image Compression
388 With Modulated Autoencoder. *IEEE Signal Processing Letters* **27**:331-335.

- 389 **H. Luo. 2017.** Hyperspectral image classification using metric learning in one-dimensional
390 embedding framework. *IEEE J. Sel. Topics Appl. Earth Observ. Remote Sens.* **10(5)**:1987-
391 2001.
- 392 **Hongchun Qu, Jian Zheng, Xiaoming Tang. 2022.** Effects of loss function and data sparsity
393 on smooth manifold extraction with deep model. *Expert Systems With Applications* **198**:1-
394 10.
- 395 **H. Tao, C. Hou, F. Nie. 2016.** Effective Discriminative Feature Selection With Nontrivial
396 Solution. *IEEE Transactions Neural Network Learning System* **27(4)**:796-808.
- 397 **J. Gui, Z. Sun, S. Ji. 2018.** Feature Selection Based on Structured Sparsity: A Comprehensive
398 Study. *IEEE Transactions Neural Network Learning System* **28 (7)**:1490-1507.
- 399 **Jian Zheng, Hongchun Qu, Zhaoni Li, Lin Li, Xiaoming Tang. 2022.** An irrelevant attributes
400 resistant approach to anomaly detection in high-dimensional space using a deep hyper
401 sphere structure. *Applied Soft Computing* **116** :1-20.
- 402 **J. Mei, M. Liu, H. R. Karimi. 2014.** Logdet divergence-based metric learning with triplet
403 constraints and its applications. *IEEE Transaction Image Process.* **23(11)**:4920-4931.
- 404 **K. Sun, S. H. Huang, D. S. Wong. 2017.** Design and Application of a Variable Selection
405 Method for Multilayer Perceptron Neural Network With LASSO. *IEEE Transactions*
406 *Neural Networks Learning System* **28(6)**:1386-1396.
- 407 **Kunjin Chen, Jun Hu, Jinliang He. 2018.** A Framework for Automatically Extracting
408 Overvoltage Features Based on Sparse Autoencoder. *IEEE Transactions on Smart Grid*
409 **9(2)**:594-604.
- 410 **Lin Feng, Huibing Wang, Bo Jin. 2019.** Learning a Distance Metric by Balancing KL-
411 Divergence for Imbalanced Datasets. *IEEE Transactions on Systems, Man, and*
412 *Cybernetics: Systems* **49(12)**:2384-2395.
- 413 **L. Theis, W. Shi, A. Cunningham. 2017.** Lossy image compression with compressive
414 autoencoders. *In Proc. Int. Conf. Learn. Representations.*1-19.
- 415 **L. Wang, Y. Wang, Q. Chang. 2016.** Feature selection methods for big data bioinformatics: A
416 survey from the search perspective. *Methods* **111**:21-31.
- 417 **Marco Capó, Aritz Pérez, Jose A. Lozano. 2021.** A Cheap Feature Selection Approach for the
418 K-Means Algorithm. *IEEE Transactions on Neural Networks and Learning Systems* **32(5)**:
419 2195-2208
- 420 **Mariucci E, Reiß M. 2017.** Wasserstein and total variation distance between marginals of Levy
421 processes. *ArXiv*:1710.02715.
- 422 **M. Luo, F. Nie, X. Chang. 2018.** Adaptive Unsupervised Feature Selection With Structure
423 Regularization. *IEEE Transactions Neural Network. Learning System* **29(4)**:944-956.
- 424 **Na Lei, Kehua Su, Li Cui. 2019.** A geometric view of optimal transportation and generative
425 model. *Computer Aided Geometric Design* **68**:1-28.
- 426 **P. Zadeh, R. Hosseini, S. Sra. 2016.** Geometric mean metric learning. *In Proc. Int. Conf. Mach.*
427 *Learning.* 2464- 2471.

- 428 **R. Hettiarachchi, J. F. Peters. 2015.** Multi-manifold lle learning in pattern recognition. *Pattern*
429 *Recognition* **48(9)**:2947-2960.
- 430 **Rami Al-Hmouz, Witold Pedrycz, Abdullah Balamash. 2022.** Logic-Oriented Autoencoders
431 and Granular Logic Autoencoders: Developing Interpretable Data Representation. *IEEE*
432 *Transactions on Fuzzy Systems* **30(3)**:869-877.
- 433 **R. Chakraborty, N. R. Pal. 2015.** Feature Selection Using a Neural Framework With
434 Controlled Redundancy. *IEEE Transactions Neural Network Learning System* **26(1)**:35-50.
- 435 **R. De Maesschalck, D. Jouan-Rimbaud, D. L. Massart. 2000.** The Mahalanobis distance,
436 Chemometrics Intell. Lab. System **50(1)**:1-18.
- 437 **S. Ying, Z. Wen, J. Shi. 2018.** Manifold preserving: An intrinsic approach for semisupervised
438 distance metric learning. *IEEE Transaction. Neural Networks Learning System* **29(7)**:
439 2731-2742.
- 440 **T. X. Pham, P. Siarry, H. Oulhadj. 2019.** A multi-objective optimization approach for brain
441 MRI segmentation using fuzzy entropy clustering and region-based active contour methods.
442 *Magn. Reson. Image* **61**:41-65.
- 443 **Ugochukwu Ejike Akpudo, Jang-Wook Hur. 2020.** Intelligent Solenoid Pump Fault Detection
444 based on MFCC Features, LLE and SVM. *2020 International Conference on Artificial*
445 *Intelligence in Information and Communication (ICAIIIC)*. 1-3.
- 446 **Weining Lu, Yu Cheng, Cao Xiao. 2017.** Unsupervised Sequential Outlier Detection with Deep
447 Architectures. *IEEE Transactions on Image Processing* **26(9)**:4321-4330.
- 448 **Xue, B., Zhang, M., Browne. 2015.** A Survey on Evolutionary Computation Approaches to
449 Feature Selection. *IEEE Transactions on Evolutionary Computation* **20(4)**:606-626.
- 450 **Zhiqiang Wan, Haibo He, Bo Tang. 2018.** A Generative Model for Sparse Hyperparameter
451 Determination. *IEEE Transactions on Big Data* **4(1)**:2-10.

Figure 1

The structure of the proposed m-AE

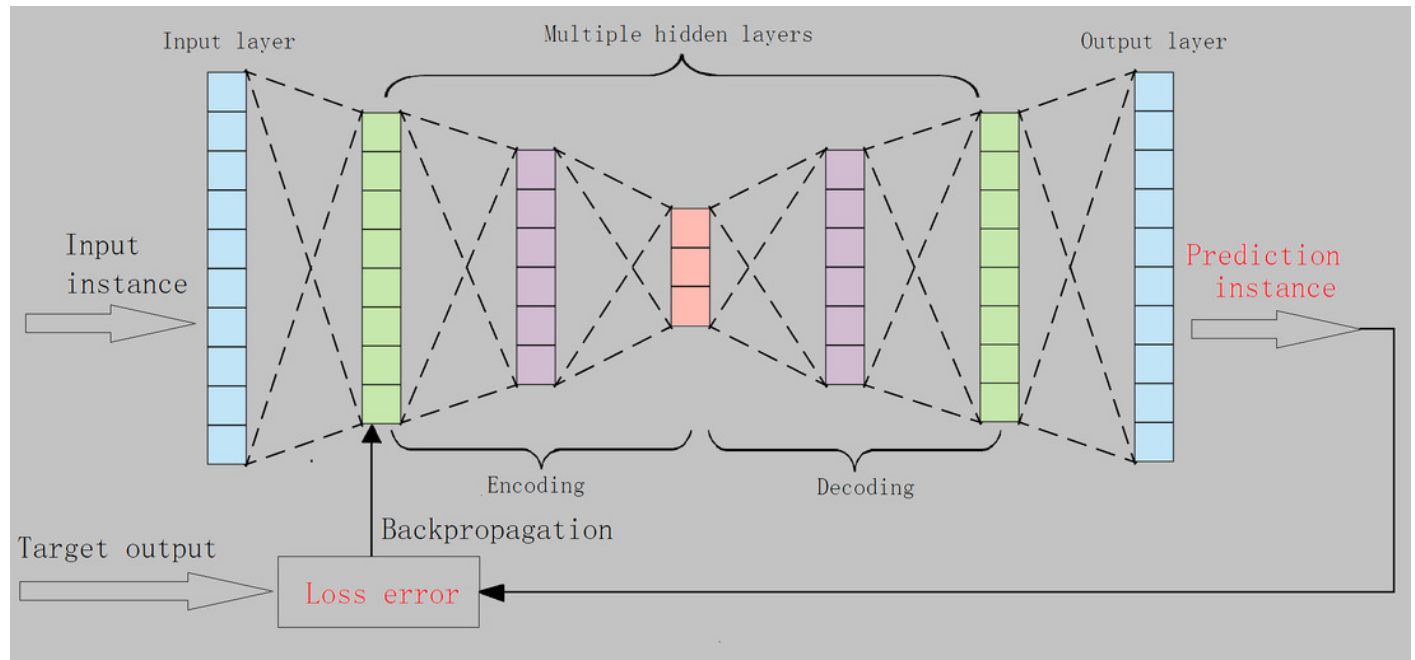


Figure 2

Validation of robustness for the proposed m-AE

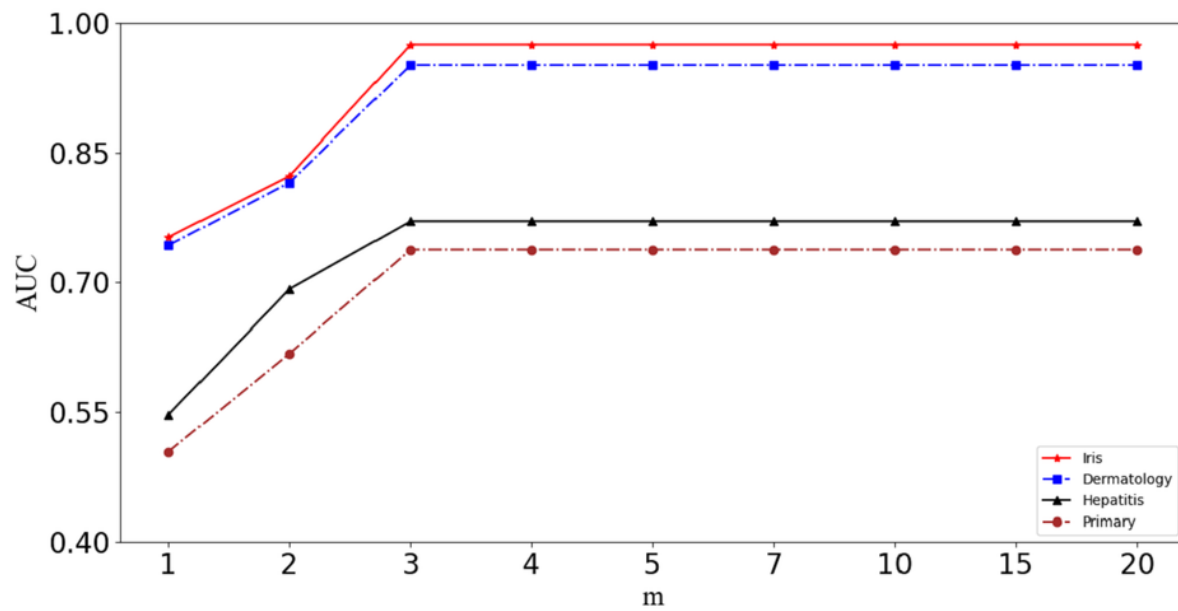


Figure 3

Validation of robustness for benchmark model AE-BK

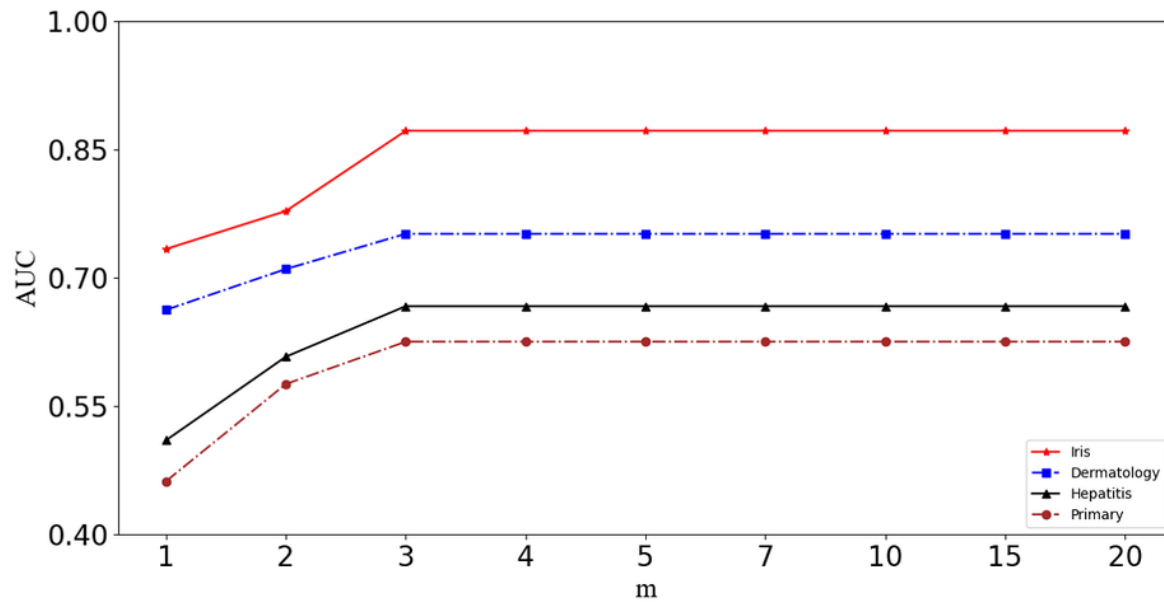


Figure 4

Results of ablation experiments

Comparisons between with distance metrics and without distance metrics. The models with distance metrics are marked as the symbol \checkmark . The models without both distance metrics and feature selection are marked as the symbol \times .

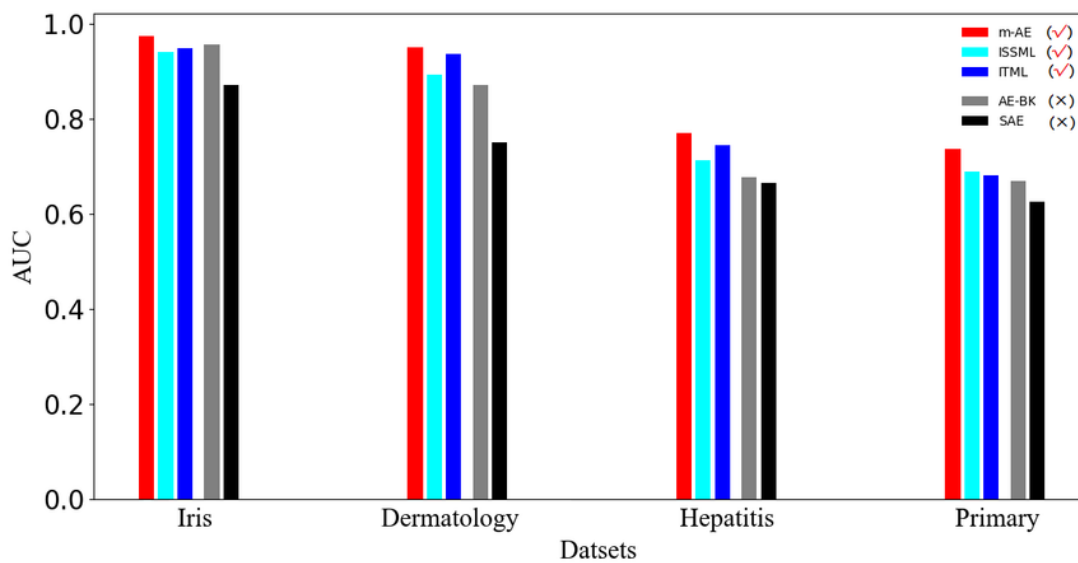


Figure 5

Results of ablation experiments

Comparisons between with distance metrics and with feature selection. The models with distance metrics are marked as the symbol \checkmark . The models with feature selection are marked as the symbol \neq .

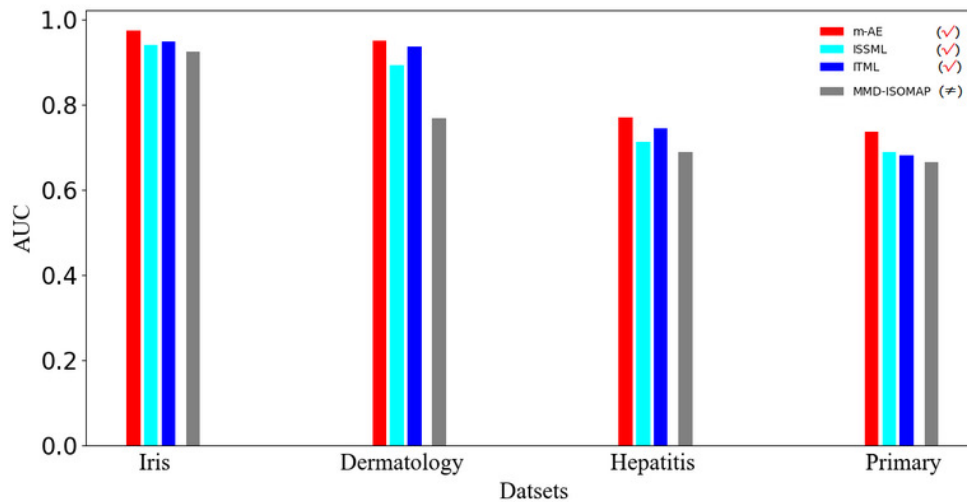


Figure 6

Visualization distributions.

The different extracted features are marked with different shapes and colors. The models with distance metrics are marked as the symbol \checkmark . The models with feature selection are marked as the symbol \neq . The models without both distance metrics and feature selection are marked as the symbol \times .

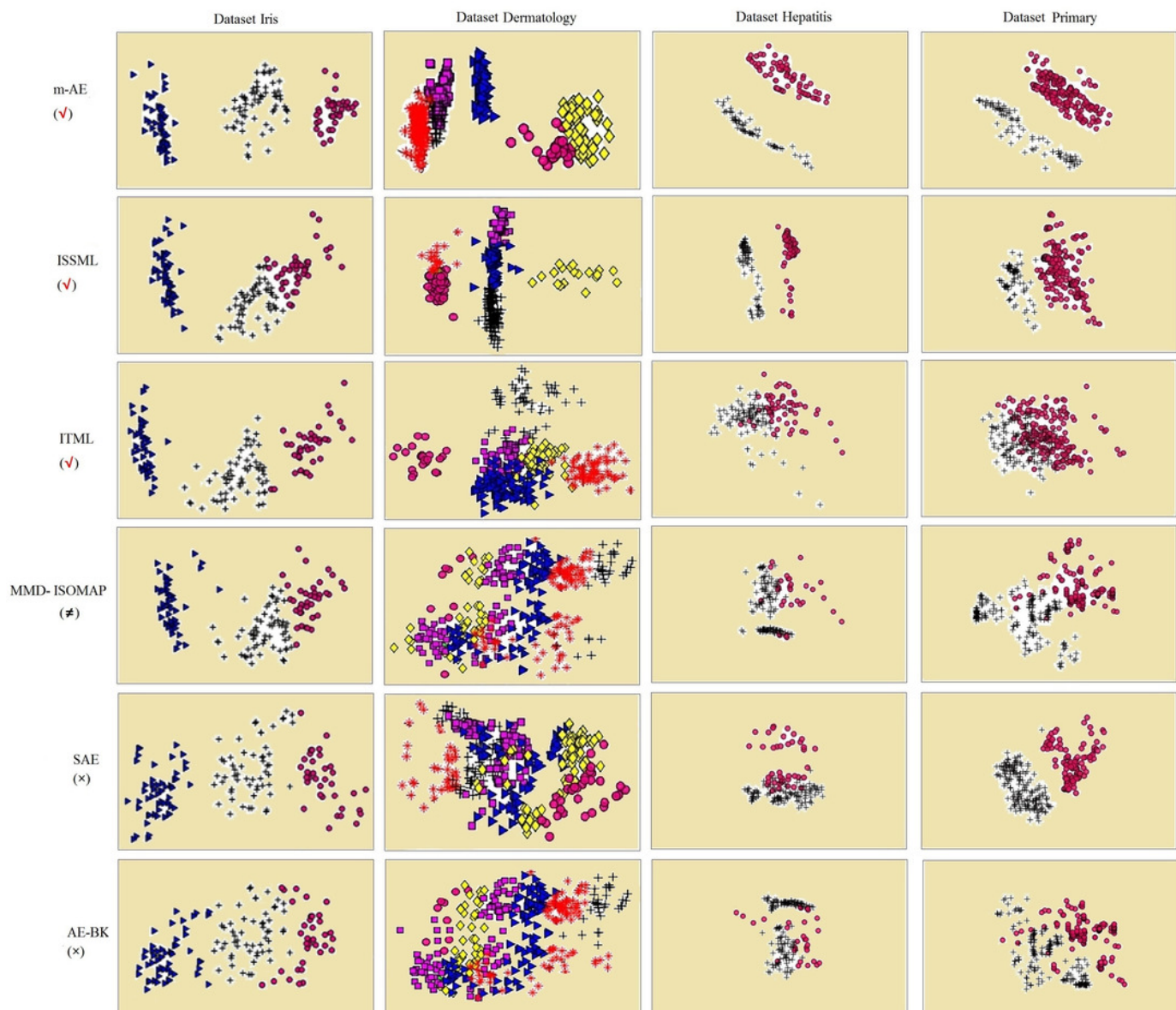
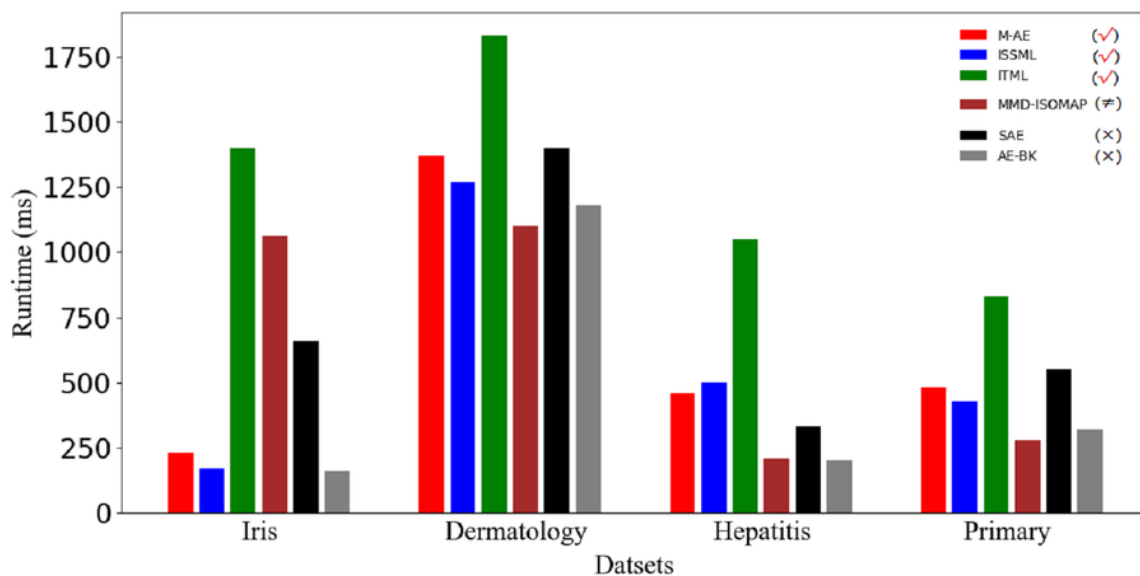


Figure 7

Runtime of methods.

The models with distance metrics are marked as the symbol \checkmark . The models with feature selection are marked as the symbol \neq . The models without both distance metrics and feature selection are marked as the symbol \times .



The models with distance metrics are marked as the symbol \checkmark . The models with feature selection are marked as the symbol \neq . The models without both distance metrics and feature selection are marked as the symbol \times .

Table 1 (on next page)

Benchmark datasets

1

Dataset	Data volume	Data dimensionality	features
Iris	150	4	3
Primary	339	17	2
Hepatitis	155	19	2
Dermatology	366	33	6

2

Table 2 (on next page)

Accuracy of feature extraction.

The best accuracy for each dataset is shown in bold. The models using a distance metric are marked as the symbol \checkmark . The models using feature selection are marked as the symbol \neq .

The models without both a distance metric and feature selection are marked as the symbol \times .

1

		Iris	Dermatology	Hepatitis	Primary
m-AE	(✓)	0.9744 ± 0.0157	0.9506 ± 0.0137	0.7703 ± 0.0753	0.7375 ± 0.0534
ISSML	(✓)	0.9402 ± 0.0154	0.8931 ± 0.0284	0.7131 ± 0.0642	0.6886 ± 0.0865
ITML	(✓)	0.9488 ± 0.0120	0.9374 ± 0.0246	0.7457 ± 0.0622	0.6816 ± 0.0745
MMD-ISOMAP (≠)		0.9247 ± 0.0053	0.7680 ± 0.0377	0.6897 ± 0.0657	0.6664 ± 0.0733
SAE	(×)	0.9571 ± 0.0227	0.8707 ± 0.0892	0.6773 ± 0.0373	0.6700 ± 0.0166
AE-BK	(×)	0.8715 ± 0.1533	0.7511 ± 0.0099	0.6666 ± 0.0771	0.6252 ± 0.1052

2